



## Structure of the mite-transmitted *Blackcurrant reversion nepovirus* using electron cryo-microscopy

Jani J.T. Seitsonen<sup>a</sup>, Petri Susi<sup>b</sup>, Anne Lemmetty<sup>c</sup>, Sarah J. Butcher<sup>a,\*</sup>

<sup>a</sup> Institute of Biotechnology, P.O. Box 65 (Viikinkaari 1), FIN-00014 University of Helsinki, Finland

<sup>b</sup> Department of Virology, University of Turku (Kiinamylynkatu 13), FIN-20520 Turku, Finland

<sup>c</sup> MTT Agrifood Research Finland, Plant Protection, FIN-31600 Jokioinen, Finland

### ARTICLE INFO

#### Article history:

Received 2 April 2008

Returned to author for revision

21 April 2008

Accepted 5 May 2008

Available online 16 June 2008

#### Keywords:

Blackcurrant reversion nepovirus

CryoEM

Three-dimensional structure

### ABSTRACT

*Blackcurrant reversion nepovirus* (BRV; genus *Nepovirus*) has a single-stranded, bipartite RNA genome surrounded by 60 copies of a single capsid protein (CP). BRV is the most important mite-transmitted viral pathogen of the *Ribes* species. It is the causal agent of blackcurrant reversion disease. We determined the structure of BRV to 1.7 nm resolution using electron cryo-microscopy (cryoEM) and image reconstruction. The reconstruction reveals a pseudo  $T=3$  viral capsid similar to that of tobacco ringspot virus (TRSV). We modelled the BRV capsid protein to that of TRSV and fitted it into the cryoEM reconstruction. The fit indicated that the extended C-terminus of BRV-CP is located on the capsid surface and the N-terminus on the interior. We generated peptide antibodies to two putatively exposed C-terminal sequences and these reacted with the virus. Hence homology modelling may be useful for defining epitopes for antibody generation for diagnostic testing of BRV in commercial crops.

© 2008 Elsevier Inc. All rights reserved.

### Introduction

Blackcurrant reversion disease (BRD) is the most important disease in blackcurrant crops (*Ribes nigrum* L.) and is caused by a plant pathogenic virus, *Blackcurrant reversion nepovirus* (BRV; ICTVdb code 00.018.0.03.031.) (Fauquet and Mayo, 1999; Lemmetty et al., 1997). BRD occurs in almost all countries where blackcurrants are grown commercially. These include countries in Eastern and Central Europe, Scandinavia, UK, Russia and New Zealand (Jones, 2000), and it is also a quarantine pathogen in many countries, which restricts the easy import of germplasm material e.g. into the US. The *Nepovirus* genus, to which BRV belongs, contains mainly nematode-transmitted viruses. BRV is the only known mite-transmitted member of the genus. It is transmitted by the eriophyid mite, *Cecidophyopsis ribis*, itself a serious pest of blackcurrant. Eriophyids were first recognized as a plant disease vector in connection with BRD (Thresh, 1964).

Most mite-transmitted plant viruses are helical viruses belonging to the *Potyviridae* family and are spread by different mite species than BRV. In contrast, BRV is a small, icosahedral nepovirus with a bipartite, plus-sense RNA genome encoding a single capsid protein (55 kDa) (Latvala-Kilby and Lehto, 1999; Latvala et al., 1998; Lemmetty et al., 1997; Mayo and Robinson, 1996). Most preparations of BRV particles purified from indicator plants (*C. quinoa* or *N. benthamiana*) are composed of two coat proteins of 54 and 55 kDa in size (Latvala et al., 1998; Lemmetty et al., 1997) with identical N-termini (Latvala et al.,

1998). Virus preparations containing only the smaller fragment (54 kDa) can be used to infect indicator plants (*C. quinoa*) by mechanical abrasion. The resulting progeny viruses contain both protein forms.

There is one described nepovirus structure, that of tobacco ringspot virus (TRSV) (Chandrasekar and Johnson, 1998; Singh et al., 1995). TRSV has a pseudo  $T=3$  capsid made up of 60 copies of a single capsid protein, 513 amino acid residues in length. It has structural similarities to both comoviruses and picornaviruses (Chandrasekar and Johnson, 1998). The capsid protein is made up of three  $\beta$ -barrel domains. It has not yet been possible to confirm the identity of the epitopes required for nematode transmission, but a few conserved residues have been identified that cluster together in two areas of the capsid surface (Chandrasekar and Johnson, 1998). Little is known about the BRV epitopes required for mite transmission.

The complexity of the transmitting agent, growth requirements, woody nature of blackcurrants and lack of sensitive detection techniques have seriously hampered the identification of BRV in commercial plants. The first functional *in vitro* assay for BRV detection was based on a combination of nucleic acid-specific detection and virus capture using antibodies with moderate specificity in an immuno-capture reverse transcriptase polymerase chain reaction (Latvala et al., 1997; Lemmetty et al., 1997; Lemmetty and Lehto, 1999). However, the development of a direct serological assay has not been reported mainly due to a lack of high specificity antisera (Susi et al., 1998).

The aim of the current work was to determine the three-dimensional model of BRV using electron cryo-microscopy (cryoEM) and three-dimensional image reconstruction (Adrian et al., 1984; Fuller

\* Corresponding author. Fax: +358 9 191 59930.

E-mail address: [sarah.butcher@helsinki.fi](mailto:sarah.butcher@helsinki.fi) (S.J. Butcher).

et al., 1996), verify the homology to other nepoviruses, generate a homology model and finally to use this to localize possible antigenic and mite-transmission determinants within the quaternary structure.

## Results

Purified, vitrified BRV was inspected by cryoEM (Adrian et al., 1984) revealing mainly RNA-filled capsids approximately 29 nm in diameter although occasionally empty capsids were also found (Fig. 1a). The structure of RNA-filled BRV capsids was solved to 1.7 nm resolution (Fig. 1b) using cryoEM and image processing techniques (Baker et al., 1999; Fuller et al., 1996; Ji et al., 2006; Marinescu and Ji, 2003). The particle has a diameter of 27 nm facet to facet and 32 nm vertex to vertex (Fig. 1c). A central section of the reconstruction revealed that the RNA is icosahedrally ordered at high radius, closely following the capsid shell. The signal from the RNA is nearly as strong as the signal from the protein shell (Fig. 1c).

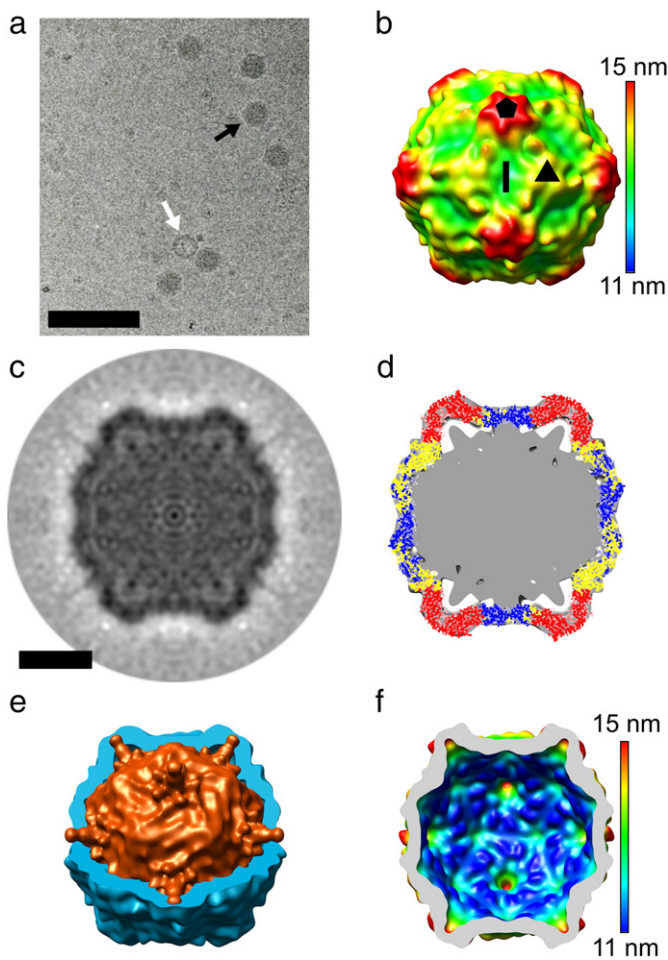


**Fig. 1.** Architecture of BRV. (a) Electron cryomicrograph of BRV at 3  $\mu\text{m}$  underfocus. An intact particle (black arrow) and an empty particle (white arrow) are indicated. The scale bar represents 100 nm. (b) Isosurface representation of the BRV reconstruction at 1.7 nm resolution. The surface is radially depth-cued as indicated by the scale bar. The symmetry axes are marked with a pentagon (five-fold), triangle (three-fold) and bar (two-fold). (c) Central cross-section of the BRV reconstruction showing the highly organized RNA. The scale bar represents 10 nm. (d) Cross-section through an isosurface representation of the BRV reconstruction (grey) with the superimposed TRSV atomic model (PDB-ID 1A6C) revealing a good fit between the two viruses. TRSV structural protein is coloured by domain: domain A (red), domain B (yellow) and domain C (blue). (e) Composite representation of the BRV protein capsid (blue) and RNA (orange). The capsid has been cut open to reveal the highly organized RNA inside. (f) Isosurface representation of the inside of the BRV capsid after the RNA has been removed, illustrating the complementarity of the capsid and RNA surfaces. The surface is radially depth-cued as indicated by the scale bar.

The BRV capsid is typical of the small RNA viruses like the nepoviruses, comoviruses and picornaviruses and is most similar to the capsid of TRSV, having a similar pseudo  $T=3$  arrangement formed of 60 copies of a single capsid protein (Arnold and Rossmann, 1988; Chandrasekar and Johnson, 1998; Hendry et al., 1999). The atomic model of TRSV (Chandrasekar and Johnson, 1998) was fitted into the BRV reconstruction (Fig. 1d) and a difference map was calculated. The major difference was the appearance of the ordered BRV RNA (Fig. 1e). The RNA complements the shape of the inside of the capsid to the extent that the RNA even protrudes into the cavities in the five-fold vertices of the capsid (Figs. 1c–f). Only small differences were seen between the TRSV and BRV capsid densities. To interpret these, we aligned the amino acid sequences of BRV with TRSV and 13 other nepoviruses (Fig. 2) and made a homology model of the BRV capsid protein (Fig. 3). These indicated that the BRV has a deletion of four amino acids in the BC loop (TRSV residues 363–366, LKPD), a three amino acid insertion in the DE loop of the C-terminal A domain (BRV residues 416–418, KAG) and a C-terminal extension of 19 amino acids. The BC and DE loop changes account for the minor differences that were seen in the turrets that occupy the vertices (Fig. 1d, 2 and 3).

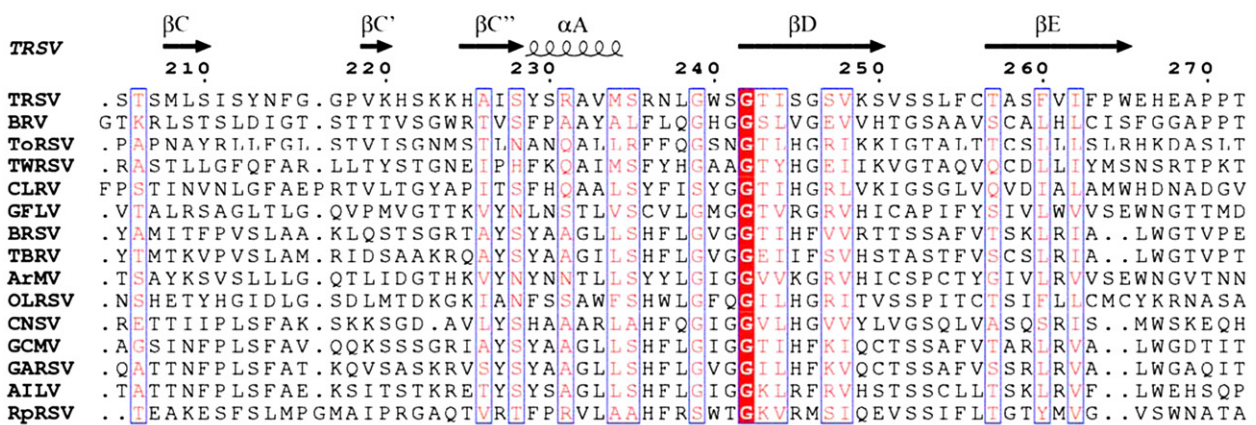
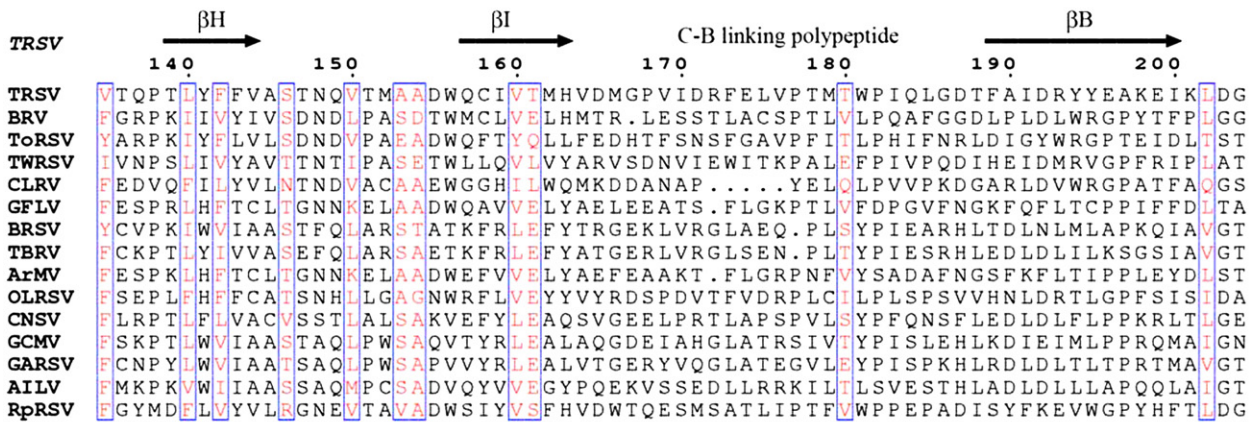
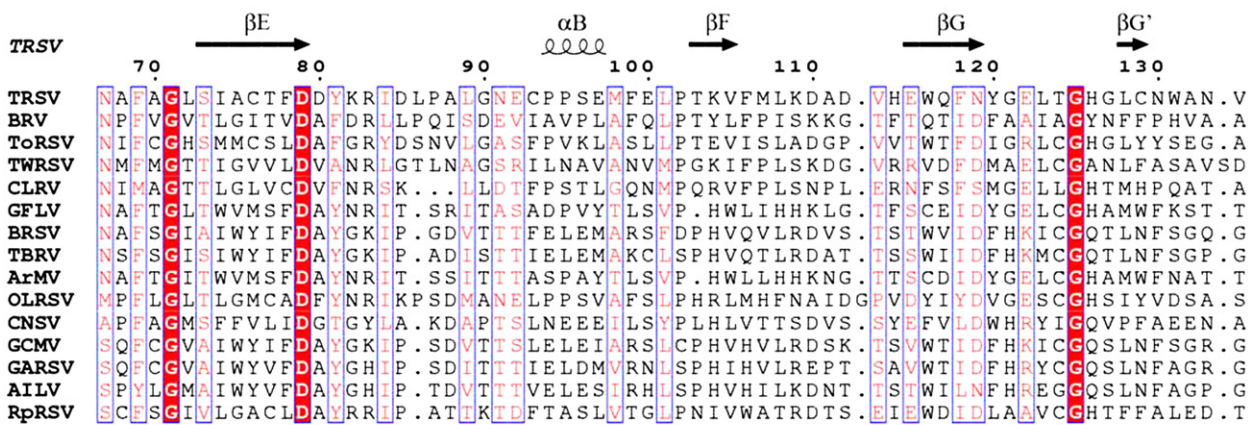
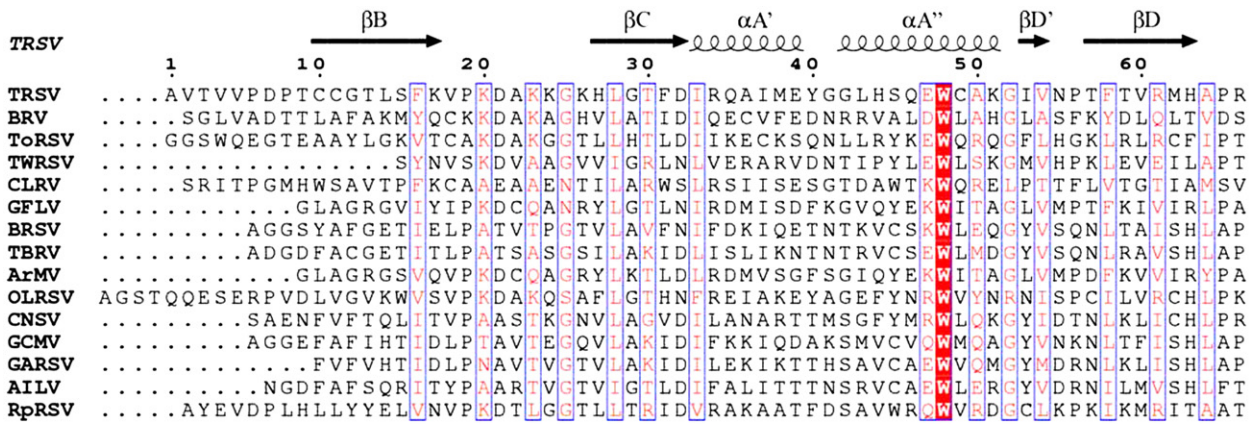
The homology model of BRV was used (Fig. 3) to map RNA–protein interactions and to identify potential antigenic sites on the quaternary structure. The BRV homology model (Figs. 3c) thus obtained fitted the cryoEM reconstruction well (Fig. 3d). The only major difference between the BRV homology model and the reconstruction is the BRV C-terminal 14 residues which project out from the surface of the virus (Fig. 3d). As the last 19 C-terminal residues are not present in TRSV this is probably one of the least reliable regions of the model. However, this is also a potential specific antigenic site as the C-terminal 19 residues are some of the least conserved in the sequence alignment (Fig. 2). Further experiments were carried out to check the antigenicity of the C-terminus (see below). The model also predicts that the N-terminal domain of the BRV capsid protein extends into the capsid interior to interact with the RNA (Fig. 3e).

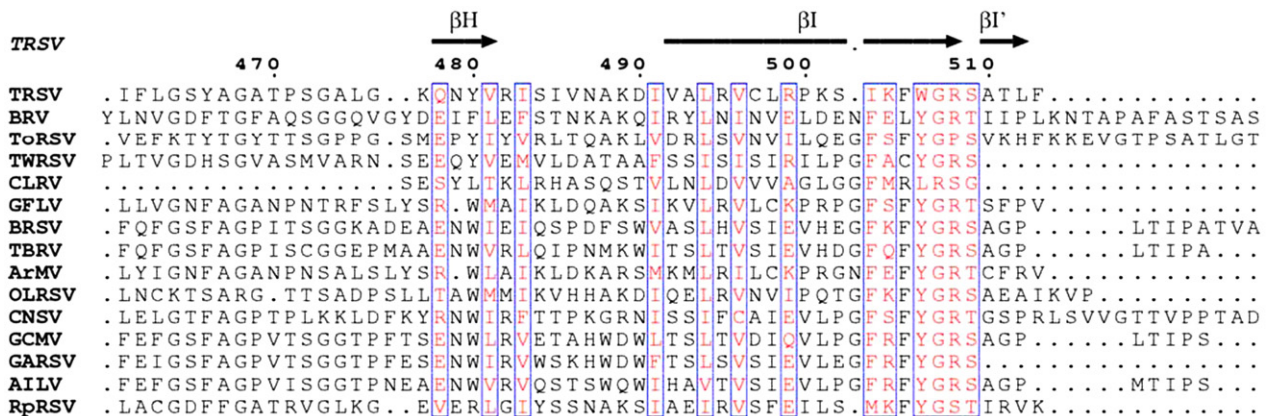
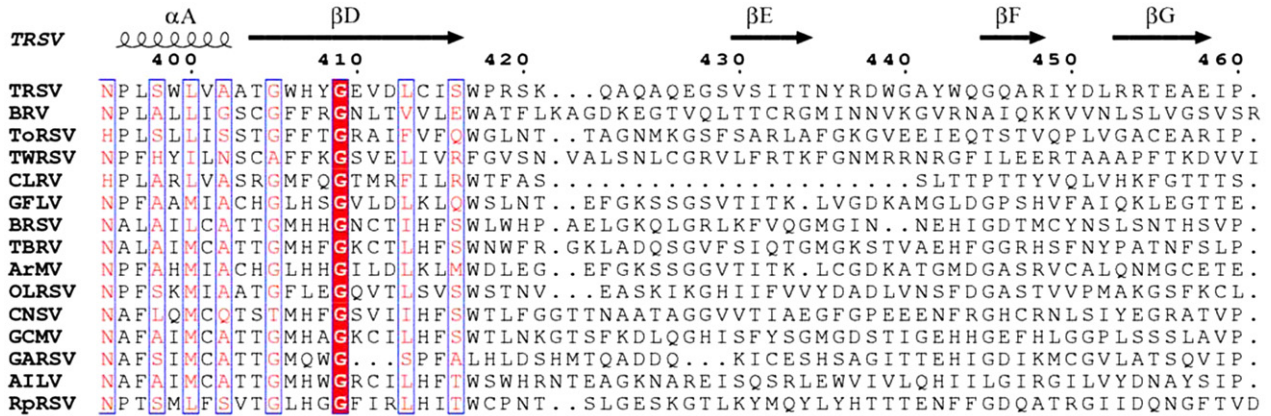
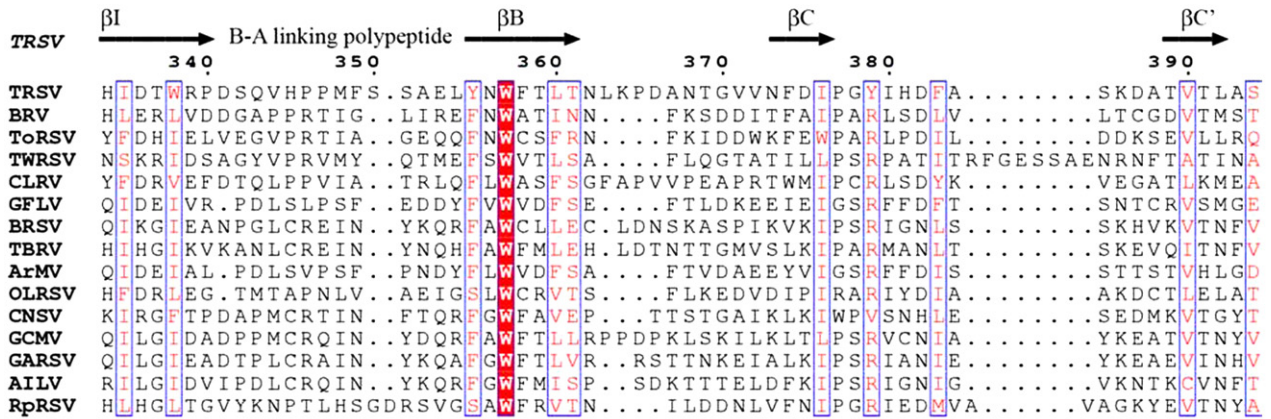
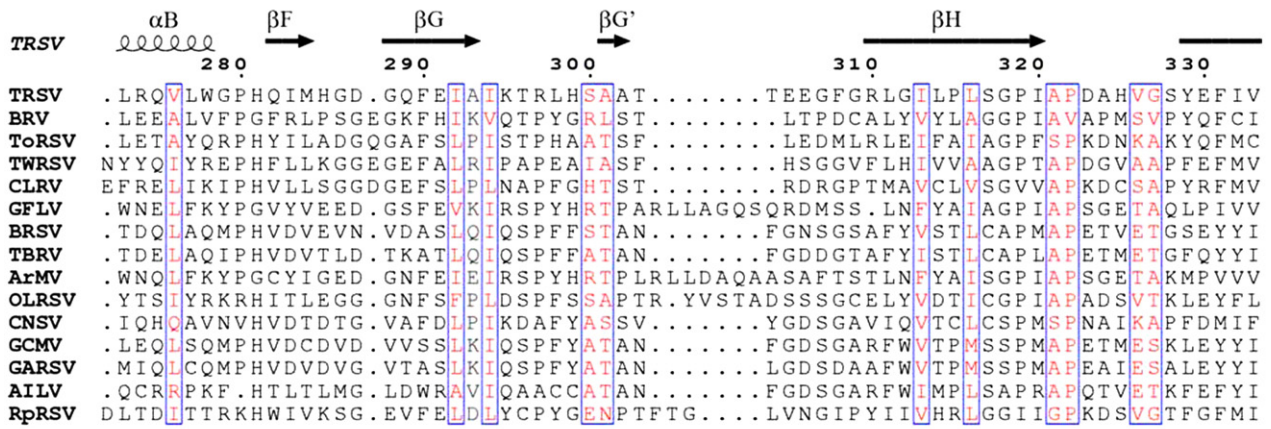
From the sequence alignment and the homology model, the largest insertion in a BRV surface-exposed loop compared to the other nepoviruses is the KAG insert in the domain A DE loop (BRV residues 416–418; Fig. 2). Due to its proximity to the five-fold vertex, multiple copies of this sequence cluster together (Fig. 3c). Hence, this could be a possible mite-transmission epitope along with the C-terminus. A second KAG sequence (BRV residues 22–24) is present near the three-fold and is part of the conserved region identified for many nepoviruses (Chandrasekar and Johnson, 1998).

To test the antigenicity of the C-terminus, three antisera were made, one against denatured BRV-CP (Ab-BRV-CP) and two against putative surface-exposed epitopes, Ab-KAK (peptide antiserum against amino acids 483–494, EFSTNKAKQIRY) and Ab-ST5 (peptide antiserum against the amino acids 524–533, ST5ASAPNES). BRV samples were then blotted onto polyvinylidene difluoride membranes and individual strips were incubated with the different antisera and shown to bind to the capsid protein (Fig. 4). The proteolytically cleaved capsid protein, seen in some virus preparations, migrating slightly faster than the full-length in SDS-PAGE, bound to both Ab-KAK and Ab-BRV-CP but not to Ab-ST5. Hence this smaller form has a C-terminal truncation. This may arise during infection or the purification process.

## Discussion

Our cryoEM studies have shown that BRV has a remarkably well organized RNA whose shapes closely mimic those of the protein capsid. This kind of highly ordered RNA packing is not commonly seen in animal viruses although it has been seen in some plant viruses (Fox et al., 1998; Wikoff et al., 1997) and invertebrate nodaviruses (Tihova et al., 2004). The high order of the genome reflects a high number of interactions between the RNA and capsid proteins. Provided that these





## TRSV

TRSV	.....
BRV	APNES.....
ToRSV	NNPVGRRPENVDTGGPGGQYAAALQAAQQAGKNPFRGR
TWRSV	.....
CLRv	.....
GFLV	.....
BRV	DVSAVSGS.....
TBRV	.....
ArMV	.....
OLRSV	.....
CNSV	ASTSNSQGGDEDIGDQYSAAALGRGRGRGSRPGPSPIRG
GCMV	.....
GARSV	.....
AILV	.....
RpRSV	.....

**Fig. 2.** Amino acid sequence comparison of nepovirus capsid proteins. Secondary structure of the TRSV atomic model compared to a clustal W alignment of the capsid proteins of TRSV (NP\_919039), BRV (NP\_612586), tomato ringspot virus (ToRSV; NP\_620762), tomato white ringspot virus (TWRSV; ABM65096), cherry leaf roll virus (CLRv; AAB27443), grapevine fanleaf virus (GFLV; NP\_619706), beet ringspot virus (BRV; NP\_620113), tomato black ring virus (TBRV; NP\_758518), arabis mosaic virus (ArMV; YP\_053924), olive latent ringspot virus (OLRSV; CAB90217), cycas necrotic stunt virus (CNSV; NP\_620620), grapevine chrome mosaic virus (GCMV; NP\_619704), grapevine Anatolian ringspot virus (GARSV; AAQ56596), artichoke Italian latent virus (AILV; CAA60707) and raspberry ringspot virus (RpRSV; NP\_944488). Fig. was created in ESPRIPT (Gouet, Robert, and Courcelle, 2003).

interactions co-operate in the assembly process, it may be that BRV assembly is more sensitive to mutations in RNA and capsid proteins than assembly of mammalian picornaviruses where the RNA is generally not as well ordered. The organization of the RNA may also indicate a potential RNA release site for infection. The cavity underneath the five-fold is occupied by the genome indicating that RNA would be capable of moving through the five-fold portal were it opened. The five-fold is known to be the release channel for at least some small, icosahedral RNA plant viruses such as cowpea chlorotic mottle virus (Speir et al., 1995).

Homology modelling of the BRV capsid was used to identify potential sequences that could be used for mite interaction. The two most obvious are the C-terminal 19 residues and the unconserved DE loop in the C-terminal A domain. It has previously been shown that virus preparations containing the shorter form of the capsid protein are infectious by mechanical abrasion, resulting in symptoms identical to BRV symptoms (Lemmetty et al., 1997). Here we show that the shorter form is due to a C-terminal truncation. Thus, the C-terminus is not important for the infectivity of the virus but may indeed serve as a determinant for mite transmission.

When considering suitable epitopes for the generation of diagnostic antibodies against BRV, various antigenic determinants must be located not only on the surface of capsid protein but also on the surface of BRV virions. The homology model of the BRV capsid predicts that the C-terminus is extended from the virion surface, and is thus suitable for antibody generation. Antibodies generated against synthetic peptides targeting the C-terminal portion of BRV capsid protein were functional indicating that C-terminus may be used for generation of antibodies for serological assays.

A knowledge of the structure of virus particles is of interest when trying to identify the virus using specific antibodies or in understanding the interactions of the virus e.g. with the host plant and transmitting vectors. The surface epitopes of only some icosahedral plant viruses have been investigated in detail using peptide scanning methods (He et al., 1998; Jaegle et al., 1988; Joisson et al., 1993; Mackenzie and Tremaine, 1986). Structural prediction methods can, therefore, provide an interesting avenue for exploring virus structure and antigenicity. The programs used in the course of this study produced comparable results which correspond reasonably well with the cryoEM-derived model. Models obtained by predictive methods can offer a quick indication of potential surface-exposed antigens on

viral capsids and thus may be of help in separating valid antigenic targets from invalid ones for diagnostic purposes.

The development of a sensitive and reliable antigenic peptide for BRV combined with regular tests would allow the recognition of the disease long before the symptoms become evident. Early detection might help in containment of the disease as diseased plants could rapidly be separated from the healthy ones and possibly before mites have the chance to spread the disease further. This kind of testing scheme could alleviate the economic impact of BRV on blackcurrant crops all over the world.

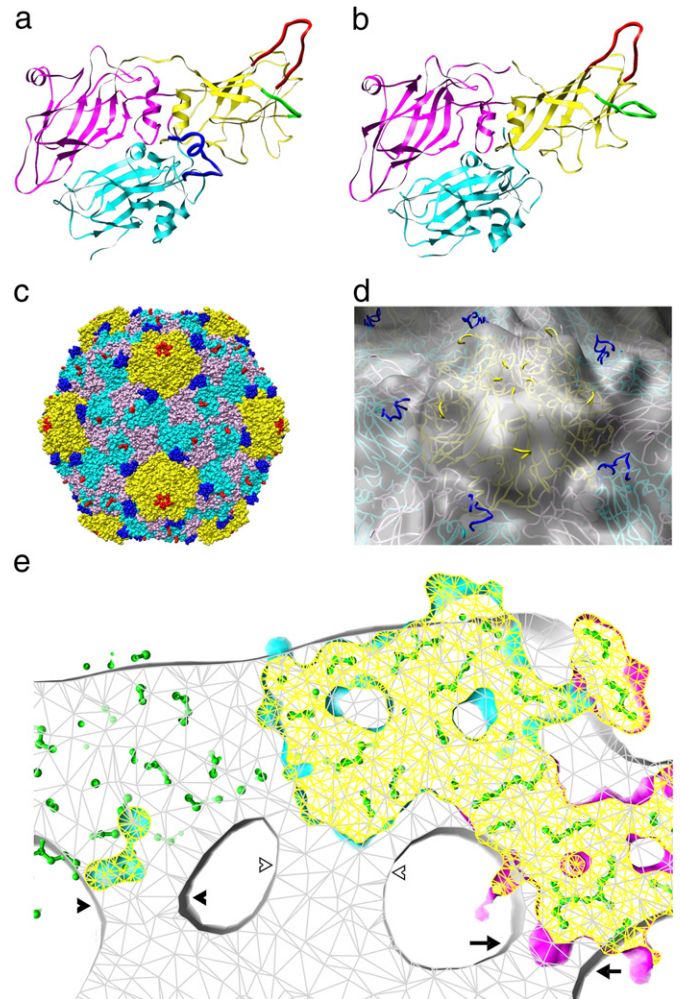


**Fig. 3.** (a) Ribbon representation of the BRV capsid protein homology model. The C-terminal 19 amino acids (blue) are indicated. Domain A loops BC (green) and DE (red) are indicated. (b) The TRSV X-ray structure shown as a ribbon model (PDB-ID: 1A6C). Domain A loops BC (green) and DE (red) are indicated. (c) Space-filling representation of the quaternary structure of the BRV homology model showing the clustering of the possible mite-specific C-terminus (blue) and KAG epitopes (red). (d) Close-up of the five-fold vertex of the BRV reconstruction (grey transparent isosurface) with the BRV homology model fitted in. The C-terminal 19 amino acids are indicated in blue sticking out of the reconstruction. In (a–d) the capsid protein is divided into three domains as follows: domain A (yellow; C-terminal segment), domain B (magenta; middle segment) and domain C (cyan; N-terminal segment). (e) A close-up of a slab of the BRV reconstruction (grey with the capped surfaces in grey mesh) with the BRV homology model fitted into the density showing the main connections between the capsid protein and RNA. The outside of the capsid is at the top; one of the capsid proteins is shown as a van der Waals surface representation with the capping surface shown as yellow mesh, domain B as magenta and C as cyan. Other copies of the capsid protein are shown as stick-and-ball models in green. Three RNA–protein interaction sites are indicated: N-terminal residues 1–3 (SGL; black arrowheads), A domain residues 112–114 (TFT; white arrowheads) and B domain residues 290–292 (FHI; black arrows).

## Materials and methods

### Purification

Inoculated and systematically infected *Chenopodium quinoa* Willd. leaves were ground up in phosphate buffer (0.05 M Na<sub>2</sub>HPO<sub>4</sub>, 0.02 M ascorbic acid, 0.02 M 2-mercaptoethanol, pH 8.0). The solution was clarified through cheese cloth and centrifuged (15 000 ×g, 20 min, 4 °C). The supernatant was adjusted to pH 5 with HCl, incubated overnight at 4 °C and clarified by centrifugation (15 000 ×g, 20 min, 4 °C). The virus was precipitated by adding 8% PEG6000 (w/v) to the supernatant and stirred for 1 h at 4 °C before being pelleted (15 000 ×g, 20 min, 4 °C). The PEG pellet was dissolved in 0.05 M Na-citrate buffer (pH 7), stirred and cleared (15 000 ×g, 20 min, 4 °C). The resulting supernatant (supernatant 1) was stored whilst the pellet was resuspended a second time and cleared once more (15 000 ×g, 20 min, 4 °C) to release additional virus (supernatant 2). Supernatants 1 and 2 were pooled and then pelleted by high speed centrifugation (105 000 ×g, 90 min, 4 °C). The pellet was resuspended and subjected to rate zonal centrifugation (10–40% sucrose in 0.05 M Na-citrate, pH 7, 164 000 ×g, 150 min, 4 °C). The gradient was fractionated, the fractions containing the virus were diluted, pelleted (180 000 ×g, 120 min, 4 °C), resuspended and stored at –80 °C in 0.05 M Na-citrate buffer (pH 7.0) until use.

### Preparation of vitrified specimens and electron microscopy

The vitrified samples were prepared from 3 µl aliquots of purified virus on Protochips C-Flat 224 grids as previously described (Baker, Olson, and Fuller, 1999). The micrographs were recorded using a GATAN 626 cryo-holder maintained at –180 °C and a FEI Tecnai F20 microscope operated at 200 kV. The images were recorded using a Gatan Ultrascan 4000 CCD camera at a nominal magnification of 68 000× and on Kodak SO163 film at a nominal magnification of 50 000×. Low dose conditions were used at all times. The sampling of the CCD camera is 15 µm. At the magnification used, this results in a nominal sampling of 0.221 nm/pixel in the digital micrographs. Comparison with the TRSV X-ray model revealed the effective magnification to be around 66 400× and the corresponding sampling to be 0.226 nm/pixel. Film micrographs were scanned using a Zeiss Photoscan TD scanner using a step size of 7 µm and binned to

14 µm. Scaling to the TRSV X-ray model resulted in a sampling of 0.292 nm/pixel.

### Image processing

Digital micrographs were inspected by eye for crystalline ice and then evaluated by determining the CTF of each micrograph. Images containing drift or astigmatism were not processed further. Particles were picked automatically using the program ETHAN (Kivioja et al., 2000), inspected by eye and extracted with EMAN (Ludtke et al., 1999). The orientation search was done with PFT2 (Baker and Cheng, 1996; Fuller et al., 1996) and POR (Ji et al., 2006). The reconstruction was done with EM3DR2 (Marinescu and Ji, 2003). The data set used consisted of 831 particles with defocus values ranging from 1.6 µm to 4.6 µm. The resolution of the model was assessed using the FSC 0.5 criteria (van Heel and Harauz, 1986). Visualization of the model was done with CHIMERA (Pettersen et al., 2004).

### Modelling of BRV capsid protein and construction of virions

Predictions of the BRV capsid protein structure were obtained using internet based homology modelling tools. The BRV capsid protein amino acid sequence (NP\_612586) was submitted to I-TASSER (Zhang, 2007) as a single chain. The I-TASSER model was aligned with the TRSV capsid protein (PDB-ID: 1A6C) using CHIMERA (Pettersen et al., 2004). Using the resulting coordinates, a complete capsid was constructed using the VIPERDB oligomer generator (Shepherd et al., 2006).

### Polyclonal and peptide antisera

Polyclonal antisera against denatured BRV capsid protein (Ab-BRV-CP) were generated in rabbits. Viral capsid protein fragments from preparative SDS-PAGE gels, were mixed and emulsified with Freund's incomplete adjuvant with a syringe, and inoculated subcutaneously into white rabbits. Two boosters were given every 14 days. The final bleed was collected and maintained at –20 °C. Anti-rabbit peptide antisera were generated against the C-terminal peptides of BRV capsid protein (EFSTNKAKQIRY [Ab-KAK] and STSASAPNES [Ab-STS] corresponding to the amino acids 482–493 and 523–533 in the capsid protein sequence, respectively), which were linked to keyhole limpet haemocyanin (Sigma-Genosys Ltd.; Cambridge, U.K.).

### Western blot

10% SDS-PAGE gels (Laemmli, 1970) were run and proteins were transferred to polyvinylidenedifluoride membranes. Membranes were blocked in 25 mM Tris-HCl, pH 7.5, 200 mM NaCl, 3% non-fat milk powder for 30 min and incubated overnight with primary antibody. On the following day, membranes were washed twice with 25 mM Tris-HCl, pH 7.5, 200 mM NaCl for 15 min each, and subjected to secondary antibody (Anti-rabbit Ig HRP-linked whole antibody, Amersham) for 2 h, washed as before and incubated for a minute in HRP-ECL enhancer solution. Membranes were exposed to X-ray film for 5–30 min.

### Acknowledgments

We thank Ilpo Weijola and Pasi Laurinmäki for excellent technical assistance and helpful discussions and the Electron Microscopy Unit, Institute of Biotechnology, Helsinki University for providing facilities. The work was supported by the Academy of Finland Centre of Excellence Programme in Virus Research (2006–2011; 1213467 to SJB), Sigrid Juselius Foundation and the Finnish Cultural Foundation (P.S.). J.J.T.S. is a Ph.D. fellow of the National Graduate School in Informational and Structural Biology.

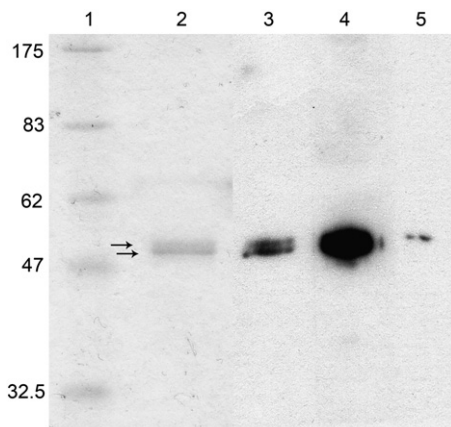


**Fig. 4.** Antibody binding to BRV capsid protein. BRV capsid proteins from sucrose-gradient-purified virus were separated on SDS-PAGE and either stained with Coomassie Brilliant Blue (lanes 1 and 2), or subjected to antibody binding (lanes 3–5). Molecular weight markers are indicated in lane 1 (Prestained Protein Marker Broad Range, New England Biolabs). Two forms of BRV capsid protein fragments are seen with Coomassie Brilliant Blue at 54 and 55 kDa indicated by the two black arrows (lane 2). Both bands react with the peptide antisera Ab-KAK (lane 3) and polyclonal antisera to BRV capsid protein (Ab-BRV-CP; lane 4), but only the longer forms react with the very C-terminal peptide antisera Ab-STS (lane 5).

## References

- Adrian, M., Dubochet, J., Lepault, J., McDowell, A.W., 1984. Cryo-electron microscopy of viruses. *Nature (London)* 308, 32–36.
- Arnold, E., Rossmann, M.G., 1988. The use of molecular-replacement phases for the refinement of the human rhinovirus 14 structure. *Acta Crystallogr. A* 44, 270–282.
- Baker, T.S., Cheng, R.H., 1996. A model-based approach for determining orientations of biological macromolecules imaged by cryoelectron microscopy. *J. Struct. Biol.* 116, 120–130.
- Baker, T.S., Olson, N.H., Fuller, S.D., 1999. Adding the third dimension to virus life cycles: three-dimensional reconstruction of icosahedral viruses from cryo-electron micrographs. *Microbiol. Mol. Biol. Rev.* 63, 862–922.
- Chandrasekar, V., Johnson, J.E., 1998. The structure of tobacco ringspot virus: a link in the evolution of icosahedral capsids in the picornavirus superfamily. *Structure* 6, 157–171.
- Fauquet, M.C., Mayo, M.A., 1999. Abbreviations for plant virus names — 1999. *Arch. Virol.* 144, 1249–1273.
- Fox, J.M., Wang, G., Speir, J.A., Olson, N.H., Johnson, J.E., Baker, T.S., Young, M.J., 1998. Comparison of the native CCMV virion with in vitro assembled CCMV virions by cryoelectron microscopy and image reconstruction. *Virology* 244, 212–218.
- Fuller, S.D., Butcher, S.J., Cheng, R.H., Baker, T.S., 1996. Three-dimensional reconstruction of icosahedral particles—the uncommon line. *J. Struct. Biol.* 116, 48–55.
- Gouet, P., Robert, X., Courcelle, E., 2003. ESPript/ENDscript: extracting and rendering sequence and 3D information from atomic structures of proteins. *Nucleic Acids Res.* 31, 3320–3323.
- He, X., Liu, S., Perry, K.L., 1998. Identification of epitopes in cucumber mosaic virus using a phage-displayed random peptide library. *J. Gen. Virol.* 79, 3145–3153.
- Hendry, E., Hatanaka, H., Fry, E., Smyth, M., Tate, J., Stanway, G., Santti, J., Maaronen, M., Hyypia, T., Stuart, D., 1999. The crystal structure of coxsackievirus A9: new insights into the uncoating mechanisms of enteroviruses. *Structure* 7, 1527–1538.
- Jaegle, M., Briand, J.P., Burckard, J., Van Regenmortel, M.H., 1988. Accessibility of three continuous epitopes in tomato bushy stunt virus. *Ann. Inst. Pasteur., Virol.* 139, 39–50.
- Ji, Y., Marinescu, D.C., Zhang, W., Zhang, X., Yan, X., Baker, T.S., 2006. A model-based parallel origin and orientation refinement algorithm for cryoTEM and its application to the study of virus structures. *J. Struct. Biol.* 154, 1–19.
- Joisson, C., Kuster, F., Plaue, S., Van Regenmortel, M.H., 1993. Antigenic analysis of bean pod mottle virus using linear and cyclized synthetic peptides. *Arch. Virol.* 128, 299–317.
- Jones, A.T., 2000. Black currant reversion disease—the probable causal agent, eriophyid mite vectors, epidemiology and prospects for control. *Virus Res.* 71, 71–84.
- Kivioja, T., Ravantti, J., Verkhovsky, A., Ukkonen, E., Bamford, D., 2000. Local average intensity-based method for identifying spherical particles in electron micrographs. *J. Struct. Biol.* 131, 126–134.
- Laemmli, U.K., 1970. Cleavage of structural proteins during the assembly of the head of bacteriophage T4. *Nature* 227, 680–685.
- Latvala-Kilby, S., Lehto, K., 1999. The complete nucleotide sequence of RNA2 of blackcurrant reversion nepovirus. *Virus Res.* 65, 87–92.
- Latvala, S., Susi, P., Lemmetty, A., Cox, S., Jones, A.T., Lehto, K., 1997. Ribes host range and erratic distribution within plants of blackcurrant reversion associated virus provide further evidence for its role as the causal agent of reversion disease. *Ann. Appl. Biol.* 131, 283–295.
- Latvala, S., Susi, P., Kalkkinen, N., Lehto, K., 1998. Characterization of the coat protein gene of mite-transmitted blackcurrant reversion associated nepovirus. *Virus Res.* 53, 1–11.
- Lemmetty, A., Lehto, K., 1999. Successful back-inoculation confirms the role of black currant reversion associated virus as the causal agent of reversion disease. *Eur. J. Plant Pathol.* 105, 297–301.
- Lemmetty, A., Latvala, S., Jones, A.T., Susi, P., McGavin, W.J., Lehto, K., 1997. Purification and properties of a new virus from black currant, its affinities with nepoviruses, and its close association with black currant reversion disease. *Phytopathology* 87, 404–413.
- Ludtke, S.J., Baldwin, P.R., Chiu, W., 1999. EMAN: semiautomated software for high-resolution single-particle reconstructions. *J. Struct. Biol.* 128, 82–97.
- Mackenzie, D.J., Tremaine, J.H., 1986. The use of a monoclonal-antibody specific for the N-terminal region of southern bean mosaic virus as a probe of virus structure. *J. Gen. Virol.* 67, 727–735.
- Marinescu, D.C., Ji, Y., 2003. A computational framework for the 3D structure determination of viruses with unknown symmetry. *J. Parallel Distrib. Comput.* 63, 738–758.
- Mayo, M.A., Robinson, D.J., 1996. Nepoviruses: molecular biology and replication. In: Harrison, B.D., Murrant, A.F. (Eds.), *The Plant Viruses Vol. 5: Polyhedral Virions and Bipartite RNA Genomes*. Plenum Press, New York, USA, pp. 139–186.
- Petersen, E.F., Goddard, T.D., Huang, C.C., Couch, G.S., Greenblatt, D.M., Meng, E.C., Ferrin, T.E., 2004. UCSF chimera—a visualization system for exploratory research and analysis. *J. Comput. Chem.* 25, 1605–1612.
- Shepherd, C.M., Borelli, I.A., Lander, G., Natarajan, P., Siddavanahalli, V., Bajaj, C., Johnson, J.E., Brooks III, C.L., Reddy, V.S., 2006. VIPERdb: a relational database for structural virology. *Nucleic Acids Res.* 34, D386–D389.
- Singh, S., Rothnagel, R., Prasad, B.V., Buckley, B., 1995. Expression of tobacco ringspot virus capsid protein and satellite RNA in insect cells and three-dimensional structure of tobacco ringspot virus-like particles. *Virology* 213, 472–481.
- Speir, J.A., Munshi, S., Wang, G., Baker, T.S., Johnson, J.E., 1995. Structures of the native and swollen forms of cowpea chlorotic mottle virus determined by X-ray crystallography and cryo-electron microscopy. *Structure* 3, 63–78.
- Susi, P., Ziegler, A., Torrance, L., 1998. Selection of single-chain variable fragment antibodies to black currant reversion associated virus from a synthetic phage display library. *Phytopathology* 88, 230–233.
- Thresh, J.M., 1964. Association between black currant reversion virus and its gall mite vector, (*Phytoptus ribis* Nal.). *Nature* 202, 1085–1087.
- Tihova, M., Dryden, K.A., Le, T.V., Harvey, S.C., Johnson, J.E., Yeager, M., Schneemann, A., 2004. Nodavirus coat protein imposes dodecahedral RNA structure independent of nucleotide sequence and length. *J. Virol.* 78, 2897–2905.
- van Heel, M., Harauz, G., 1986. Resolution criteria for three dimensional reconstruction. *Optik* 73, 119–122.
- Wikoff, W.R., Tsai, C.J., Wang, G., Baker, T.S., Johnson, J.E., 1997. The structure of cucumber mosaic virus: cryoelectron microscopy, X-ray crystallography, and sequence analysis. *Virology* 232, 91–97.
- Zhang, Y., 2007. Template-based modeling and free modeling by I-TASSER in CASP7. *Proteins* 69, 108–117.